Layered Oxide Polymer Nanocomposites: Synthesis, Characterization, and Strategies for Achieving Enhanced Barrier Property

T. Hansen, P. Barber, J. Ma, H. Ploehn, and H.-C. zur Loye

University of South Carolina, Columbia, SC, USA, zurloye@mail.chem.sc.edu

ABSTRACT

A layered silicate, hectorite, was synthesized and covalently modified with a trialkoxysilane. Polymer nanocomposite films containing exfoliated hectorite platelets were prepared. Fluorescence quenching experiments were performed to determine the oxygen permeability. Preliminary results show that the hectorite nanocomposite film has an increase in the gas barrier compared to the polymer without exfoliated clay.

Keywords: polymer, nanocomposite, hectorite, gas barrier

1 INTRODUCTION

An important goal of research in the area of polymer nanocomposites is to enhance the gas barrier property of plastics for food packaging and medical applications. Since the success of Toyota's research on a Nylon-6 nanocomposite using montmorillonite clay, the focus has shifted towards nanocomposites that contain layered additives [1]. Certain polymers alone have minimal barrier for gases such as carbon dioxide, oxygen, and water vapor. Layered additives that are capable of exfoliation into platelets with high aspect ratio provide a more tortuous path for gas diffusion, and therefore improve the gas barrier [2]. However, most layered materials need to be organically modified to promote exfoliation and to improve compatibility with the polymer.

We have synthesized various layered oxides including layered clays, perovskites, phosphonates, and polysilicates in order to prepare several layered oxide polymer nanocomposites [3]. Currently, the vast majority of polymer nanocomposites contain raw clays, such as montmorillonite, that are ion-exchanged with quaternary ammonium salts or other swelling agents [2,4-12]. Synthetic oxides offer several advantages over raw clays, since their composition is controlled, and in some cases, they can be modified *in situ*. For example, Carrado and coworkers have developed a method to covalently functionalize hectorite clay during the synthesis with organotrialkoxysilanes [9]. Using this method, we have incorporated silanes into the syntheses to alter the hydrophobicity of the hectorite surface.

Since the synthesis of hectorite has been established, requires only mild conditions, and is relatively inexpensive, hectorite is a good candidate for a polymer nanocomposite additive. Hectorite is also thermally stable, easy to exfoliate, and has aspect ratios comparable to montmorillonite.

Hectorite, having an ideal composition of $[Ex_{0.66}Si_8(Mg_{5.34}Li_{0.66})O_{20}(OH,F)_4]$ (where Ex. is an exchangeable cation), is a smectite clay mineral consisting of two tetrahedral silicate sheets with a central magnesium-oxygen octahedral layer. Isomorphous substitution of lithium for magnesium in the octahedral layer causes an overall negative charge of the layers balanced by interlayer hydrated cations.

In this study, modified and unmodified hectorite was synthesized and exfoliated. The resulting platelets were incorporated into polymer films to examine the nanocomposite properties, including oxygen permeation.

2 EXPERIMENTAL

2.1 Hectorite Synthesis

Hectorite is synthesized according to previously published methods [13]. A typical synthesis consists of a slurry of LiF, Mg(OH)2, and silica sol in water refluxed for 48-72 hours. The product is obtained after centrifugation, washing several times with DI water, and drying in air.

To covalently modify the hectorite synthesis *in situ*, the silica source, is replaced with a trialkoxysilane, such as phenyltriethoxysiliane (PTES).

Both unmodified and modified samples of hectorite are characterized by X-ray diffraction (XRD) and thermal gravimetric analysis (TGA). The presence of organic groups on the surface of the hectorite layers is also confirmed by fourier transform infrared (FTIR) spectroscopy

2.2 Polymer Film Preparation

Hectorite is first dispersed into water and stirred vigorously while heating (80-90ºC) overnight. The resulting suspension is centrifuged to remove the largest unexfoliated platelets. The supernatant is then heated and stirred for 2 hours, and centrifuged again to remove any remaining unexfoliated platelets. Complete exfoliation is confirmed by transmission electron microscopy (TEM). Size distribution of exfoliated hectorite platelets is determined from dynamic light scattering (DLS), while platelet thickness and distribution is determined using atomic force microscopy (AFM).

Films are prepared by adding a certain amount of polymer into the exfoliated hectorite suspension, so that the

desired weight percent of clay to polymer is achieved. Typically, polyvinyl alcohol (PVA), or other water soluble polymer is added to the hectorite suspension. The suspension is stirred while heating until the polymer/clay mixture is transparent and well dispersed. The final weight percentage of hectorite to polymer is 5-10%, although higher clay loadings were achieved. The mixture is allowed to cool to room temperature, poured into Petri dishes, and dried at 60ºC.

3 CHARACTERIZATION

X-ray powder diffraction (XRD) data were collected using a Rigaku D/Max 2200 powder diffractometer with CuKα radiation over the 2θ range of 2 -64.

Thermal analysis measurements, TGA and differential thermal analysis (DTA), were obtained from TA Instruments SDT 2960 and SDT Q600, at a heating rate of 10ºC/min to 800ºC.

FTIR measurements were made using a Shimadzu FTIR-8400 spectrometer, with a diffuse reflectance solid state attachement (Pike Technologies).

For AFM imaging, samples were diluted with acetone and dropped onto a freshly cleaved mica sheet and dried. The images were recorded with a PicoPlus AFM (Molecular Imaging) operated in the acoustically-driven, intermittent contact ("tapping") mode. AFM images were analyzed using the Scanning Probe Image Processor (SPIP) image analysis software (Image Metrology).

Samples for transmission electron microscopy (TEM) were prepared by placing a drop of the diluted platelet suspension onto the carbon coated TEM grid and allowed to air dry. TEM images were acquired on aHitachi H-8000 TEM at 200 kV accelerating voltage.

For the analysis of particle size using DLS, the platelet suspension was first diluted to 10^{-4}-10^{-5} g/L. DLS measurements were performed using a Brookhaven light scattering system, including a model BI-200 goniometer, model BI-9000AT correlator, and model Lexel 95 argon-ion laser that was operating at a wavelength of 514.5 nm.

For fluorescence quenching experiments, films containing a fluorescent dye, tris-(2,2'-bipyridine) ruthenium (II) chloride (RuBipy), were placed in a standard cuvet and measurements were taken over 14 days using a SLM AMINCO MC-200 monochromatic fluorimeter.

4 RESULTS AND DISCUSSION

4.1 Hectorite

XRD patterns for the synthesized unmodified hectorite match previously published patterns for hectorite (Figure 1). The *d*(001) basal spacing is 14.46Å, and peaks at 4.49Å and 2.56Å correspond to (110,020) and (130) hectorite reflections, respectively.

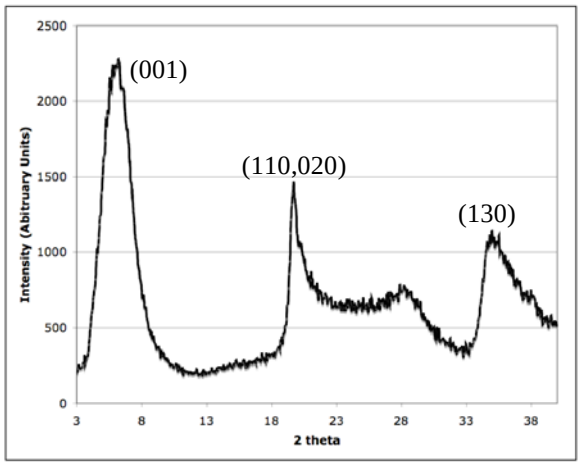

Figure 1. XRD pattern for unmodified hectorite. The *d*(001) basal spacing is 14.46Å.

For the PTES-Hectorite sample, the basal spacing decreases to 13.0Å. According to Carrado, et al., this decrease is due to the slight hydrophobicity of the layers, which would decrease the amount of water in the interlayer region, and thus decrease the interlayer spacing. Also, the phenyl rings are most likely lying flat on the hectorite surface [9].

From TGA experiments, the weight loss of hectorite in the range of 200 to 800 ºC is very small, about 3%. However, the PTES-Hectorite sample has a weight loss of 20.35% in the same temperature range, indicating the presence of organic groups (Figure 2).

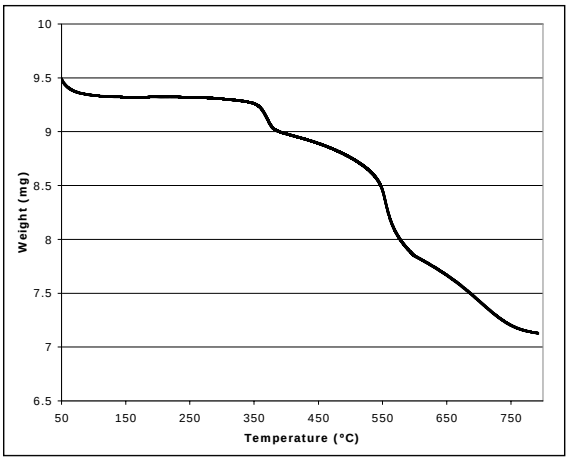

Figure 2. TGA weight loss of PTES-Hectorite.

Peak assignments from FTIR data can also be attributed to organic groups attached to the clay. Specifically, peaks at 1730, 1791, 1850, and 1920 cm^{-1} are assigned to monosubsituted benzene overtones, also confirming the presence of PTES.

The size of the individual exfoliated platelets can be determined from TEM images (Figure 3). Typical hectorite

platelets are approximately 400-500 nm, which correlates with DLS average platelet size distributions. Platelet size of the umodified and modified hectorite are similar.

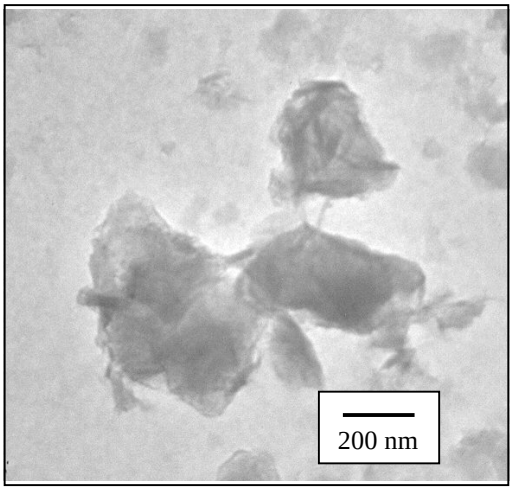

Figure 3. TEM image of hectorite platelets.

The AFM thickness distribution is shown in Figure 4. Since the majority of the thicknesses occur between 1 and 2 nm, corresponding to a single hectorite layer, the sample is well exfoliated.

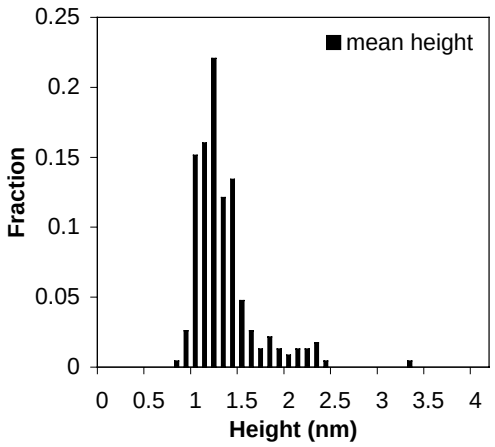

Figure 4. Height distribution of hectorite platelets.

4.2 Polymer Films

Since the hectorite platelets are already exfoliated before the addition of the polymer, clay platelets will most likely remain exfoliated or well intercalated. Films made with unexfoliated material show visible aggregates of clay under an optical microscope. However, Polymer nanocomposite films were prepared up to 30 wt. % that remain remarkably transparent with no visible aggregates, suggesting that the hectorite platelets are well dispersed and exfoliated (Figure 5).

Figure 5. Polymer film containing 30 wt. % hectorite.

4.3 Gas Barrier Measurement

Since the ultimate goal in this study was to produce nanocomposites with improved gas barrier property, we used an alternate route to determine the oxygen diffusion by fluorescence quenching experiments [14]. After the polymer was added to the exfoliated hectorite solution and dispersed, a small amount of the fluorescent dye (RuBipy) was added. The dried film fluoresced under UV light (Figure 6). A control polymer film was also prepared without clay to compare results.

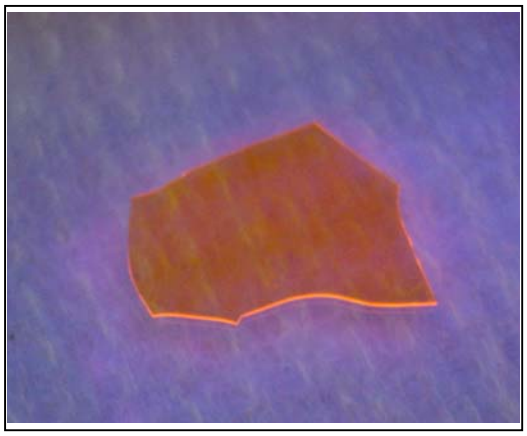

Figure 6. Polymer film containing hectorite and RuBipy.

These films were then purged with nitrogen to remove any initial oxygen from the films. Oxygen quenches the fluorescent emission of the dye, so films were then exposed again to oxygen, and the intensity was measured over time. The oxygen diffusion can be determined from the Stern-Volmer luminescence quenching equation combined with Fick's law of diffusion [14]. An oxygen penetration model was also applied to the data. From the model fit, values of the oxygen diffusion coefficients and equivalent permeabilities of the nanocomposite films are obtained. The barrier improvement factor is calculated from the ratio of

the permeability in the control film to that in the nanocomposite film.

From these results, the fluorescence of the dye in the control film is quenched at a faster rate than the rate of the hectorite nanocomposite films (Figure 7).

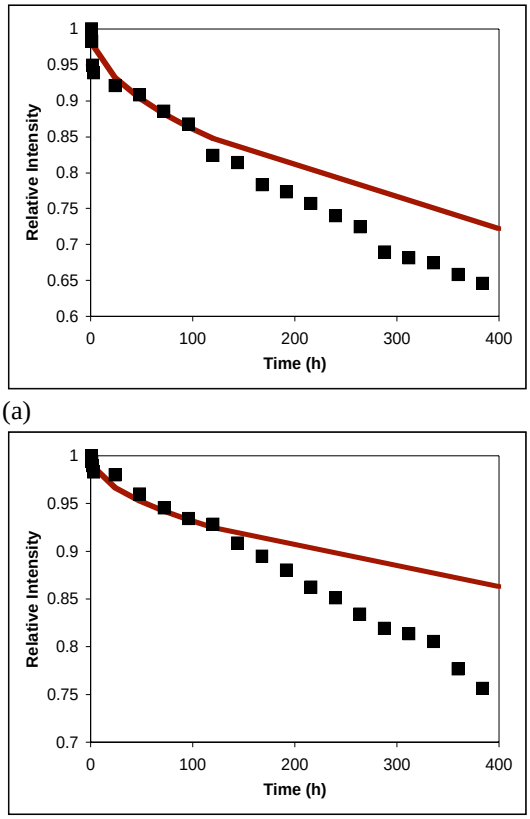

(a)

(b)

Figure 7. Relative intensities of RuBipy in the control polymer film (a) and the polymer film containing 5 wt.% hectorite (b). Red solid lines are fits of the oxygen penetration model to the data, valid at short times.

Hectorite platelets most likely create a tortuous path that prevents the oxygen from diffusing into the films, as expected. Preliminary analysis of the data shows that a 5 wt.% hectorite nanocomposite film has a barrier improvement factor (BIF) of 4, which suggests the hectorite nanocomposite has a barrier to oxygen 4 times that of the control (Figure 8). The PTES-hectorite nanocomposite film has a BIF of only 2.08. Since the polymers in this study are hydrophilic, and the PTES-hectorite is slightly hydrophobic, the unfavorable interactions might cause voids in the film, allowing the oxygen to diffuse more easily. In future studies, nanocomposites with more hydrophobic polymers, including polyethylene terephthalate, will be prepared. Hectorite and other layered oxides that have been covalently functionalized are expected to have superior gas barrier performance in polymer nanocomposites compared to the unmodified clays.

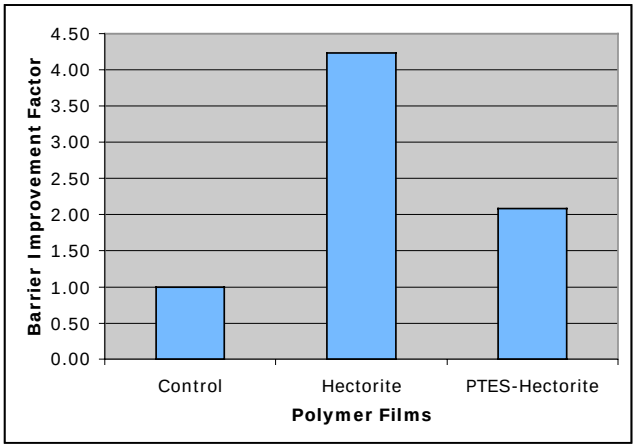

Figure 8. Calclulated barrier improvement factors for polymer nanocomposite films containing 5 wt.% clay and RuBipy.

REFERENCES

[1] A. Usuki, Y. Kojima, et al. Journal of Materials Research, 8(5), 1179-1184, 1993.

[2] T.J.Pinnavaia and G. W. Beall, " Polymer-Clay Nanocomposites," John Wiley & Sons, Ltd., 2000.

[3] H.-C. zur Loye and T.J. Hansen, "Polymer Composite Materials and Methods for Producing Same," USCRF Ref. 425 - PCT Patent Application No. PCT/US2005/026200, 2005.

[4] M. Alexandre and P. Dubois, Materials Science and Engineering R: Reports, 28, 1-63, 2000.

[5] M.Pluta. M.-A. Paul, M. Alexandre, and P. Dubois, J. of Polym. Sci. Part B: Polymer Physics, 44, 299-311, 2006.

[6] P. Ni, Q.Wang, J. Li, and J. Suo, Journal of Applied Polymer Science, 99, 6-13, 2006.

[7] P.C. LeBaron, Z. Wang,and T.J. Pinnavaia, Applied Clay Science, 15, 11-29, 1999.

[8] S.S. Ray, and M. Okamoto, Prog. Polym. Sci., 28, 1539-1641, 2003.

[9] K.A. Carrado, L. Xu, R. Csencsits, and J.V. Muntean, Chemistry of Materials , 13, 3766-3773, 2001.

[10] D.R. Paul, Q.H. Zeng, A.B. Yu, and G.Q. Lu, J. of Colloid and Interface Science, 292, 462-468, 2005.

[11] W. Gianelli, G. Ferrara, G. Camino, et al.. Polymer, 46, 7037-7046, 2005.

[12] B. Chen and J.R.G. Evans, Macromolecules, 39, 747-754, 2006.

[13] K.A. Carrado, Applied Clay Science, 17, 1-23, 2003.

[14] Y. Rharbi, A.Yekta, and M.A. Winnik, Analytical Chemistry, 71, 5045-5053, 1999.